Field Theory of Anisotropic Quantum Hall Gas

Kenzo Ishikawa (with T. Aoyama, Y. Ishizuka, and N. Maeda, H. Suzuki,

November 27, 2003

at. Komaba (Sakita)

Int. J. Mod. Phy. B17, 4765 (2003)

1 Introduction

1.1 Thomas-Fermi model and anomaly in one dimensional compressible gas

The electrons are in the smooth electrostatic potential $\delta\phi(x)$. The density vs Fermi momentum,

$$\begin{aligned} n(x) &= \int_{-p_F}^{p_F} dp \frac{1}{2\pi\hbar} \\ &= \frac{p_F}{\pi\hbar}. \end{aligned} \tag{1}$$

The constant chemical potential,

$$\frac{{p_F}^2}{2m} + e\delta\phi(x) = \mu = \frac{{p_{F0}}^2}{2m}. \tag{2}$$

Equation for the potential and Thomas-Fermi screening,

$$\begin{aligned} \frac{\partial^2}{\partial x^2}\delta\phi(x) &= -4\pi e N^{(0)}(n - n^0) \\ &= {\xi_{TF}}^2 \delta\phi(x), \\ \xi_{TF} &= (\frac{\hbar v_F}{4eN^{(0)}})^{1/2}. \end{aligned} \tag{3}$$

1.2 Schwinger model: one dimensional axial anomaly and ICDW

$$\partial_\mu F^{\mu\nu} = e j^\mu$$
$$\partial_\mu {j_5}^\mu = \frac{e}{2\pi}\epsilon_{\mu\nu}F^{\mu\nu} \quad (4)$$
$${j_5}^\mu = \epsilon_{\mu\nu} j_\nu$$

$$\partial_\mu{}^2 F = -\frac{e^2}{2\pi}F$$
$$F = \epsilon_{\mu\nu}F^{\mu\nu} \quad (5)$$

1+1 dimensional axial anomaly is equivalent to Thomas Fermi screening.- - - - - - Sakita-Z. B. Su

1.3 incompressible gas (liquid) vs compressible gas of finite quantum Hall system

() incompressible liquid

→ "no-screening" "droplet with sharpe edge" Iso-Karabali-Sakita,

() compressible Hall gas

→ "screening " "spreading gas ? "

() anisotropic quantum Hall gas(incompresible x compressible)

→ "screening or no-screening? " ?

1.4 Fine structure constant and quantum Hall effect

The fine structure constant α : the combination of e, c, h, and the dielectric constant of vacuum, ϵ_0,

$$\alpha = e^2/2\varepsilon_0 ch. \quad (6)$$

The electron's $g-2$:

Theory (Kinoshita)

$$
\begin{aligned}
g-2 &= \alpha/2\pi - 0.328478965(\alpha/\pi)^2 + 1.17562(56)(\alpha/\pi)^3 \\
&\quad +(-)1.472(152)(\alpha/\pi)^4 + 4.46\times 10^{-12}. \qquad (7)
\end{aligned}
$$

Experiment (Van Dyck et. al.)

$$g-2 = 1159652188.4(4.3)\times 10^{-12}. \qquad (8)$$

Comparison

$$\alpha_{g-2}^{-1} = 137.03599976(50)(3.7ppb) \qquad (9)$$

Quantum Hall effect

$$\alpha_{QHE}^{-1} = 137.0360037(33)(0.024ppm). \qquad (10)$$

Quantum Hall effects(Klitzing,Tsui et al): believed as,

$$
\begin{aligned}
\sigma_{xy} &= (e^2/h)n \\
\sigma_{xy} &= (e^2/h)q/p, \qquad (11) \\
\sigma_{xx} &= 0
\end{aligned}
$$

, around $\nu = n$, or q/p, where $\nu = \rho/\rho_0$. Here ρ is the electron's density and ρ_0 is the degeneracy of the Landau levels per unit area.

2 quantum Hall dynamics on von Neumann lattice

2.1 von Neumann lattice representation

One body Hamiltonian: $H_0 = (\mathbf{p} + \ e\mathbf{A})^2/2m, |rot\mathbf{A}| = B$. The classical solutions: The center (X, Y) and the velocity, $\mathbf{v}$,

$$x = v_y/\omega + X, y = -v_x/\omega_c + Y, \omega_c = eB/m \tag{12}$$

. Commutation relation (non-commutative center coordinates),

$$\begin{aligned} &[X, v_x] = [X, v_y] = [Y, v_x] = [Y, v_y] = 0, \\ &[x, y] = [v_x, v_y]/{\omega_c}^2 + [X, Y] = 0, \\ &[X, Y] = -[v_x, v_y]/{\omega_c}^2 = -i\hbar/eB. \end{aligned} \tag{13}$$

The von Neumann lattice coherent state:

$$|\alpha_{m,n}\rangle = \exp(i\pi(m + n + mn) + \pi^{1/2}(A^\dagger \frac{z_{mn}}{a} - A\frac{z_{mn}}{a}))|0\rangle, \tag{14}$$

where

$$\begin{aligned} &a = \sqrt{\frac{2\pi\hbar}{eB}}, \\ &z_{mn} = a(m\omega_x + n\omega_y), \\ &Im(\omega_x^* \omega_y) = 1, \\ &A = \frac{\sqrt{\pi}}{a}(X + iY), [A, A^\dagger] = 1, \\ &m, n = Z \end{aligned} \tag{15}$$

This complete set satisfies

$$\langle\alpha_{m+m',n+n'}|\alpha_{m',n'}\rangle = \exp(i\pi(m + n + mn) - \pi/2|\frac{z_{mn}}{a}|^2) \tag{16}$$

$$|\alpha_{\mathbf{p}}\rangle = \sum_{m,n} e^{ip_x m + ip_y n}|\alpha_{m,n}\rangle,$$
$$\langle\alpha_{\mathbf{p}}|\alpha'_{\mathbf{p}}\rangle = \gamma(\mathbf{p})\sum_N (2\pi)^2\delta(\mathbf{p} - \mathbf{p}' - 2\pi\mathbf{N}) \quad (17)$$

, $N_x, N_y = Z$, and the fundamental region of $\mathbf{p}$ is defined as, $|p_x| \leq \pi, |p_y| \leq \pi$. The normalization constant

$$\gamma(\mathbf{p}) = \beta(\mathbf{p})^*\beta(\mathbf{p}), \quad (18)$$
$$\beta(\mathbf{p}) = (2\mathrm{Im}\tau)^{\frac{1}{4}}\, e^{i\frac{\tau}{4\pi}p_y^2}\vartheta_1(\frac{p_x + \tau p_y}{2\pi}|\tau),$$

where

$$\tau = -\frac{\omega_x}{\omega_y},$$
$$\vartheta_1(z|\tau) = theta function,$$
$$\beta(\mathbf{p} + 2\pi\mathbf{N}) = e^{i\phi(\mathbf{p},\mathbf{N})}\beta(\mathbf{p}), \quad (19)$$
$$\phi(\mathbf{p},\mathbf{N}) = \pi(N_x + N_y) - N_y p_x.$$

The relative variables, (ξ, η),

$$\xi = x - X = v_y/\omega_c, \eta = y - Y = -v_x/\omega_c, \quad (20)$$

commute with the center variables, (X, Y). Eigenstates of H_0,

$$H_0|f_l\rangle = E_l|f_l\rangle. \quad (21)$$
$$E_l = \frac{eB}{m}\hbar(l + \frac{1}{2}),$$

The direct product,

$$|l, \mathbf{p}\rangle = |f_l\rangle \otimes |\alpha_{\mathbf{p}}\rangle/\beta(\mathbf{p}) \quad (22)$$

2.2 field theory

The Hamiltonian of the quantum Hall system $\mathcal{H}_0 + \mathcal{H}_{int}$

$$\begin{aligned}\mathcal{H}_0 &= \int d^2x \psi^\dagger(\mathbf{x}) H_0 \psi(\mathbf{x}),\\ \mathcal{H}_{int} &= \int d^2k \rho(\mathbf{k}) V(\mathbf{k}) \rho(-\mathbf{k})/2,\\ \rho(\mathbf{k}) &= \int d^2x e^{i\mathbf{k}\cdot\mathbf{x}} \psi^\dagger(\mathbf{x},t)\psi(\mathbf{x},t)\end{aligned} \tag{23}$$

and $V(\mathbf{k})$ is the Coulomb potential. Electron field,

$$\psi(\mathbf{x}) = \int_{\mathrm{BZ}} \frac{d^2p}{(2\pi)^2} \sum_{l=0}^{\infty} b_l(\mathbf{p}) \langle \mathbf{x}|l,\mathbf{p}\rangle. \tag{24}$$

Operators satisfy anti-commutation relations,

$$\{b_l(\mathbf{p}), b_{l'}^\dagger(\mathbf{p}')\} = \delta_{l,l'} \sum_N (2\pi)^2 \delta(\mathbf{p}-\mathbf{p}'-2\pi\mathbf{N}) e^{i\phi(\mathbf{p}',\mathbf{N})}, \tag{25}$$

and satisfy a torus boundary condition with a phase factor, $\phi(\mathbf{p},\mathbf{N})$, in the momentum space. The free Hamiltonian and density operators,

$$\mathcal{H}_0 = \sum_l \int_{\mathrm{BZ}} \frac{d^2p}{(2\pi)^2} E_l b_l^\dagger(\mathbf{p}) b_l(\mathbf{p}), \tag{26}$$

$$\begin{aligned}\rho(\mathbf{k}) &= \sum_l \int_{\mathrm{BZ}} \frac{d^2p}{(2\pi)^2} b_l^\dagger(\mathbf{p}) b_{l'}(\mathbf{p}+a\hat{\mathbf{k}}) f_{ll'}(\mathbf{k}) \exp[\frac{i}{4\pi} a\hat{k}_x(2p_y + a\hat{k}_y)],\\ \mathbf{j}(\mathbf{k}) &= \sum_l \int_{\mathrm{BZ}} \frac{d^2p}{(2\pi)^2} b_l^\dagger(\mathbf{p}) b_{l'}(\mathbf{p}+a\hat{\mathbf{k}}) \langle f_l|\frac{1}{2}\{\mathbf{v}, e^{-i(k_x\xi+k_y\eta)}\}|f_l'\rangle\\ &\quad \exp[\frac{i}{4\pi} a\hat{k}_x(2p_y + a\hat{k}_y)],\\ f_{ll'}(\mathbf{k}) &= \langle f_l|e^{-i(k_x\xi+k_y\eta)}|f_l'\rangle\end{aligned}$$

here, $\hat{k}_i = W_{ij}k_j$ with the matrix W defined by ω_x and ω_y.

2.3 Ward-Takahashi identity and the Hall conductance

With the transformed electron operators,

$$\begin{aligned}\tilde{b}_l(\mathbf{p}) &= \sum_{l'} U_{ll'}(\mathbf{p}) b_{l'}(\mathbf{p}),\\ U^\dagger_{ll'}(\mathbf{p}) &= \langle f_l | e^{i(\tilde{p}_x\xi+\tilde{p}_y\eta)/a-\frac{i}{4\pi}p_xp_y} | f_{l'}\rangle, \tilde{p}_i = W^{-1}_{ij} p_j, \end{aligned} \tag{27}$$

the density operators becomes diagonal form,

$$\begin{aligned}\rho(\mathbf{k}) &= \int_{\mathrm{BZ}} \frac{d^2p}{(2\pi)^2} \sum_l \tilde{b}^\dagger_l(\mathbf{p}) \tilde{b}_l(\mathbf{p}+a\tilde{\mathbf{k}}), \\ [\rho(\mathbf{k}), \tilde{b}_l(\mathbf{p})]\delta(t-t') &= -\tilde{b}_l(\mathbf{p}-\mathbf{k})\delta(t-t'),\end{aligned} \tag{28}$$

The vertex part $\tilde{\Gamma}^\mu$, and the propagator, $\tilde{S}$,

$$\tilde{\Gamma}_\mu(p,p) = t^\nu{}_\mu \frac{\partial \tilde{S}^{-1}(p)}{\partial p^\nu}, \tag{29}$$

where $t^\mu_\nu q^\nu$ is defined through $(q_0, a\hat{q}_x, a\hat{q}_y) = t^\mu_\nu q^\nu$. The current correlation function

$$\begin{aligned}\pi^{\mu\nu}(q,q') &= \int dx dx' e^{iqx-iq'x'} \langle T(j^\mu(x) j^\nu(x'))\rangle \\ &= (2\pi)^3 \delta(q-q') \pi^{\mu\nu}(q) + \pi^{\mu\nu}_{(2)}(q,q').\end{aligned} \tag{30}$$

The Hall conductance ,

$$\begin{aligned}\sigma_{xy} &= \frac{e^2}{3!} \epsilon^{\mu\nu\rho} \partial_\rho \pi_{\mu\nu}(q)|_{q=0}, \qquad (31)\\ &= \frac{e^2}{h} N_w, \\ N_w &= \frac{1}{24\pi^2} \int_{\mathrm{BZ}\times S^1} d^3p \epsilon_{\mu\nu\rho} \mathrm{tr}\left(\partial_\mu \tilde{S}^{-1}(p) \tilde{S}(p) \partial_\nu \tilde{S}^{-1}(p) \tilde{S}(p) \right.\\ &\quad \left. \partial_\rho \tilde{S}^{-1}(p) \tilde{S}(p)\right), \qquad (32)\end{aligned}$$

N_w = a winding number of the propagator, $\tilde{S}(p)$, and agrees with an integer if the integrand is single-valued and has no singularity. This is satisfied in the integer Hall effect and in periodic potential system.

2.4 value of topological winding number and integer quantum Hall effect

Free theory

The winding number of the propagator is stable under small changes of the systems,but depends upon the propagator and the position of Fermi energy. The value for the free propagator is computed as a function of the Fermi energy. The value stays at an integer in finite energy region and has step-like behavier as a whole. This occurs because one particle energy takes discrete values, E_l, and there is no state between these energy values in free theory.

Disorders

The **plateau** appears in the system of disorders because the topological invariant is stable under small changes of the system. By treating interactions perturbatively, the Hall conductance has plateaus at the exactly quantized values also in the system of interactions as far as the ground state is in the same phase.

Hall gas

In the system of Hall gas where one particle energy is not degenerate but has a momentum dependence,the Hall conductance is unquantized. The value changes with Fermi energy.

3 Anisotropic Hall gas state(stripe)

3.1 Broken symmetry of anisotropic quantum Hall gas (stripe)

Symmetry: the translation in y-direction Q_X, the translation in x-direction Q_Y,the rotation Q_J, and the total charge Q satisfy

$$
\begin{aligned}
&[Q,\mathcal{H}] = [Q_X,\mathcal{H}] = [Q_Y,\mathcal{H}] = [Q_J,\mathcal{H}] = 0, \\
&[Q_X,Q_Y] = \frac{i}{eB}Q, \\
&[Q_J,Q_X] = iQ_Y, [Q_J,Q_Y] = -Q_X, \\
&[Q_X,Q] = [Q_Y,Q] = [Q_J,Q] = 0.
\end{aligned} \tag{33}
$$

The total charges are obtained from Noether current.

The commutation relations between Q_X and Q_Y does not allow ,

$$Q_X|0\rangle = 0, Q_Y|0\rangle = 0 \tag{34}$$

, but

$$(Q_X + iQ_Y)|0\rangle = 0, \tag{35}$$

$$Q_X|0\rangle = q|0\rangle, Q_Y|0\rangle \neq 0 \tag{36}$$

is OK.(Laughlin ,Stripe)

In a strong magnetic field, intra Landau levels are most important. The interaction Hamiltonian ,

$$\mathcal{H}_{int} = \int d^2k\rho(\mathbf{k})v(\mathbf{k})\rho(-\mathbf{k})/2, \tag{37}$$

Symmetry:

$$b_l(\mathbf{p}) \rightarrow b_l(\mathbf{p}+\mathbf{K}), \rho(\mathbf{k}) \rightarrow e^{i(\frac{a}{2\pi}k_x)K_y}\rho(\mathbf{k}). \tag{38}$$

Quantum Hall gas → a momentum dependent one particle energy with minimaly broken **K** symmetry.

$$\langle b_l^\dagger(\mathbf{p}) b_l(\mathbf{p}') \rangle = \delta(\mathbf{p}-\mathbf{p}')\theta[p_y+\nu\pi]\theta[\nu\pi - p_y], \qquad (39)$$

The mean field Hamiltonian in the momentum space,

$$\begin{aligned} \mathcal{H}_m &= \int_{\mathrm{BZ}} \frac{d^2p}{(2\pi)^2} \epsilon_l(\mathbf{p}) b_l^\dagger(\mathbf{p}) b_l(\mathbf{p}) + E_l(0), \qquad (40) \\ \epsilon(\mathbf{p}) &= kineticenergy. \end{aligned}$$

$\mu_0(\nu)$ is a chemical potential, the self-consistency condition at ν in l-th Landau level,

$$\begin{aligned} \epsilon(\mathbf{p}) &= -\int_{\mathrm{BZ}} \frac{d^2p'}{(2\pi)^2} v_{HF}(\mathbf{p}'-\mathbf{p})\theta[\mu_0(\nu) - \epsilon(\mathbf{p}')], \\ \nu &= \int_{\mathrm{BZ}} \frac{d^2p'}{(2\pi)^2} \theta[\mu_0(\nu) - \epsilon(\mathbf{p}')]. \qquad (41) \end{aligned}$$

Solution with a p_y dependent one particle energy. Density and current density in real space become also asymmetric. The **phase factor** in the charge density is due to commutation relation between the guiding center coordinates, X and Y. It leads the density profile of the present mean field in coordinate space to be uniform in y-direction and is periodic in x-direction, hence this state agrees with unidirectional charge density wave of **Koulakov,Fogler,and Shklovskii and of Moessner and Chalker**. From the shape of **Fermi surface**, this is like the integer quantum Hall state in p_y direction ,and conductance vanishes.

3.2 Symmetry breaking and Nambu-Goldstone zero-mode

In this section we set $a = 1$. Q_Y and Q_J are broken spontaneously. Goldstone theorem in **non-commutataive coordinates** (X, Y) and spectrum of Nambu-Goldstone zero mode.

$$
\begin{aligned}
&\mathcal{H}|n\rangle = E_n|n\rangle, \\
&e^{i2\pi(Q_X/r_s L_x)}|n\rangle = e^{i2\pi(Q_X^{(n)}/r_s L_x)}|n\rangle, \qquad (42)\\
&e^{i2\pi r_s Q_Y}|n\rangle = e^{i2\pi r_s Q_Y^{(n)}}|n\rangle, \\
&Q|n\rangle = N_e|n\rangle \qquad (43)
\end{aligned}
$$

The expectation value of the algebra in the coordinate space,

$$
\frac{i}{2\pi}\partial_x\langle j^0(\mathbf{r},t)\rangle = \langle 0|[Q_Y, j^0(\mathbf{r},t)]|0\rangle = \int d\mathbf{r}'\langle 0|[j_Y^0(\mathbf{r}',t'), j^0(\mathbf{r},t)]|0\rangle, \qquad (44)
$$

The left-hand side does not depend on t, hence the energy gap, $\Delta E_{NG}(\mathbf{q})$ vanishes in the small q limit. Thus the existence of gapless excitation mode is proved.

Spectrum of Nambu-Goldstone mode by single mode approximations. Map into l-th Landau level space,

$$
\begin{aligned}
&\rho_*(\mathbf{k}) = P_l\rho(\mathbf{k})P_l = \int_{\mathrm{BZ}} \frac{d^2p}{(2\pi)^2} b_l^\dagger(\mathbf{p}) b_l(\mathbf{p} - \mathbf{a}\mathbf{k}) e^{\frac{-i}{4\pi}k_x(2p_y - k_y)}, \\
&\mathcal{H}^{(l)} = \frac{1}{2}\int \frac{d^2k}{(2\pi)^2}\rho_*(\mathbf{k}) v_l(k) \rho_*(-\mathbf{k}), \\
&v_l(k) = e^{-k^2/4\pi}[L_l(k^2/4\pi)^2 2\pi q^2/k. \qquad (45)
\end{aligned}
$$

The density operator satisfies the commutation relations,

$$[\rho_*(\mathbf{k}), \rho_*(\mathbf{k}')] = -2i\sin(\frac{\mathbf{k}\times\mathbf{k}'}{4\pi})\rho_*(\mathbf{k}+\mathbf{k}'),$$
$$[Q_X, \rho_*(\mathbf{k})] = -\frac{k_y}{2\pi}\rho_*(\mathbf{k}),$$
$$[Q_Y, \rho_*(\mathbf{k})] = \frac{k_x}{2\pi}\rho_*(\mathbf{k}), \tag{46}$$
$$|\mathbf{k}\rangle = \rho_*(\mathbf{k})|0\rangle,$$

Assume that this state is one particle state of NG mode and computes its energy from,

$$\Delta(\mathbf{k}) = \frac{\langle\mathbf{k}|(\mathcal{H}^{(l)} - E_0)|\mathbf{k}\rangle}{\langle\mathbf{k}|\mathbf{k}\rangle}. \tag{47}$$

To compute the numerator we use,

$$\langle\mathbf{k}|(\mathcal{H}^{(l)} - E_0)|\mathbf{k}\rangle = \langle 0|[\rho_*(-\mathbf{k}), \mathcal{H}^{(l)}]\rho_*(\mathbf{k})|0\rangle$$
$$= -\langle 0|[\mathcal{H}^{(l)}, \rho_*(\mathbf{k})]\rho_*(-\mathbf{k})|0\rangle, \tag{48}$$

Reflection symmetry,

$$\langle 0|\rho_*(\mathbf{k})\rho_*(-\mathbf{k})|0\rangle = \langle 0|\rho_*(-\mathbf{k})\rho_*(\mathbf{k})|0\rangle,$$
$$\langle 0|\rho_*(\mathbf{k})\mathcal{H}^{(l)}\rho_*(-\mathbf{k})|0\rangle = \langle 0|\rho_*(-\mathbf{k})\mathcal{H}^{(l)}\rho_*(\mathbf{k})|0\rangle, \tag{49}$$
$$\mathcal{H}^{(l)}|0\rangle = E_0|0\rangle.$$

The spectrum,

$$\Delta(\mathbf{k}) = [Ak_x^2 + Bk_y^4 + O(k_x^2k_y^2, k_x^4)]|k_y|. \tag{50}$$

The energy spectrum is an-isotropic and vanishes with higher powers in the small momentum region. At $k_x = 0$ the energy depends on fifth power of k_y and at a finite k_x the energy depends linearly on the magnitude of k_y.

3.3 Preferred orientation under external density modulation

Add small density modulation term of wave vector, $\mathbf{K}_{ext}$, $\mathcal{H} + \mathcal{H}_{\rm ext}$,

$$\mathcal{H}_{\rm ext} = \lambda \int d^2r\,\rho(\mathbf{r})\ cos\mathbf{K_{ext}} \cdot \mathbf{r}. \tag{51}$$

In small λ, apply perturbative expansion. The energy dependes on the angle, θ. For the small $\mathbf{K_{ext}}$, the energy becomes minimum when the angle is $\frac{\pi}{2}$. Thus the stripe is alligned perpendicular to the external modulation. This result is understandable from the shape of Fermi surface.

All the one particle states are filled in the p_x direction and Landau level energy gap. Hence the many body state is hard and does not get any perturbative energy if the external perturbation is in the x-direction.

From the energies of the both states we obtain phase diagram as a function of several parameters. In small g,**orthogonal phase** in which both direction are orthogonal is realized and in large g,**parallel phase** in which both directions are parallel is realized.

3.4 Hall conductance

From the propagator in the current basis,

$$\begin{aligned} \tilde{S}^{(c)}_{ll'}(p) &= U_{ll''}(\mathbf{p}) S^{(c)}_{l''l'''}(p) U^{\dagger}_{l'''l'}(\mathbf{p}), \\ S^{(c)}_{ll'}(p)^{-1} &= \delta_{ll'}(p_0 - (E_l + \varepsilon_l(\mathbf{p}))), \end{aligned} \tag{52}$$

We find

$$\sigma_{xy} = \frac{e^2}{h}(n + \nu'), \tag{53}$$

at $\nu = n + \nu'$.

3.5 Longitudinal resistances

The K_x-invariant anisotropic Hall gas states at $\nu = n + 1/2$ have the Fermi surface parallel to the p_x axis. The p_x direction → Landau level's energy gap. The system is like the integer quantum Hall state, $\sigma_{xx} = 0$.

The p_y direction → a bunch of parallel one-dimensional systems. In Landauer formula, the velocity

$$\begin{aligned} v_y &= \frac{\partial \varepsilon(p_y)}{\partial p_y}, \\ \Delta n &= \frac{1}{2\pi}\frac{\partial p_y}{\partial \varepsilon}\Delta\varepsilon, \\ \Delta n &= \frac{1}{2\pi}\frac{\partial p_y}{\partial \varepsilon}\Delta\varepsilon. \end{aligned} \tag{54}$$

The total current,

$$I_y = ev_y\Delta n = \frac{e^2}{2\pi}V_y, \tag{55}$$

Conductance

$$\sigma_{yy} = \frac{e^2}{h}. \tag{56}$$

The resistance is the inverse of the conductance. ρ_{xx} becomes finite and ρ_{yy} vanishes. The **easy direction** is the y direction.

4 Dielectric function, plasmon and other higher order effects

The current-current correlation function,

$$\tilde{\pi}^{\mu\nu}(\mathbf{k},\omega) = \frac{-i\int_{-\infty}^{\infty} dt_1 dt_2 \langle\Psi_0| T \mathop{\circ}\limits_{\circ} j^{\mathrm{H}\mu}(\mathbf{k},t_1) j^{\mathrm{H}\nu}(-\mathbf{k},t_2) \mathop{\circ}\limits_{\circ} |\Psi_0\rangle e^{-i\omega\cdot(t_1-t_2)}}{TS} \tag{57}$$

with the total time T and the total area S of 2D electron system is given in the RPA approximation,

$$\begin{aligned}\tilde{\pi}^{00}_{\mathrm{bubble}}(\mathbf{k},\omega) &= \pi^{(0)}_{00}(\mathbf{k},\omega) + \sum_n \pi^{(0)}_{0n}(\mathbf{k},\omega) W_n(\mathbf{k}) \pi^{(0)}_{n0}(\mathbf{k},\omega) \\ &\quad + \sum_{nm} \pi^{(0)}_{0n}(\mathbf{k},\omega) W_n(\mathbf{k}) \pi^{(0)}_{nm}(\mathbf{k},\omega) W_m(\mathbf{k}) \pi^{(0)}_{m0}(\mathbf{k},\omega) + \cdots \\ &= \sum_n \pi^{(0)}_{0n}(\mathbf{k},\omega)[1 - W(k)\pi^{(0)}(\mathbf{k},\omega)]^{-1}_{n0},\end{aligned} \tag{58}$$

where

$$\pi^{(0)}_{nm}(k_y,\omega) = -i\int_{-\infty}^{\infty}\frac{dp_0}{2\pi}\int_{\mathrm{MBZ}}\frac{dp_y}{2\pi}\ \tilde{G}^{(0)}_{p_y,p_0}\ \tilde{G}^{(0)}_{p_y+k_y,p_0+\omega}\ e^{-ip_y(n_x-m_x)}\delta_{n_y-m_y,0} \tag{59}$$

and $W_n(\mathbf{k}) \equiv V_l(\mathbf{k} + 2\pi\tilde{\mathbf{n}})$, $\mathbf{a}\times\mathbf{b} = a_x b_y - a_y b_x$. $\pi^{(0)}_{nn}$ is independent on n. Here, $\sum_n = \sum_{n=-\infty}^{+\infty}$ appears as the result of dividing the infinite momentum integral region by one MBZ.

Babble and ladder diagrams are summed up,

$$\begin{aligned}\tilde{\pi}^{00}_{\mathrm{GRPA}}(\mathbf{k},\omega) &= \pi^{(0)}_{00}(\mathbf{k},\omega) + \sum_n \pi^{(0)}_{0n}(\mathbf{k},\omega)\{W_n(k) - \tilde{W}_n(k)\}\pi^{(0)}_{n0}(\mathbf{k},\omega) \\ &+ \sum_{nm} \pi^{(0)}_{0n}(\mathbf{k},\omega)\{W_n(k) - \tilde{W}_n(k)\}\pi^{(0)}_{nm}(\mathbf{k},\omega)\{W_m(k) - \tilde{W}_m(k)\}\pi^{(0)}_{m0}(\mathbf{k},\omega) + \cdots \\ &= \sum_n \pi^{(0)}_{0n}[1 - W^{\mathrm{eff}}(k)\pi^{(0)}(\mathbf{k},\omega)]^{-1}_{n0},\end{aligned} \tag{60}$$

where we define $W_n^{\text{eff}}(k) \equiv W_n(k) - \tilde{W}_n(k)$. Here, $\tilde{W}_n \equiv \tilde{V}_l(\frac{k_y}{2\pi} + \tilde{n}_y, \frac{k_x}{2\pi} + \tilde{n}_x)$, and $\tilde{V}_l(\vec{\alpha}) = \int \frac{d^2\beta}{(2\pi)^2} V_l(\beta) e^{i\vec{\beta}\cdot\vec{\alpha}}$.

The exchange term between the electron and hole becomes negative. This GRPA is the same content given by the TDHA by Cote and Macdonald. The effective interaction $W_0^{\text{eff}}(k)$ becomes repulsive in the small k region and attractive in the large k region.

4.1 Dielectric function

In the RPA, the dielectric function

$$\epsilon^{\text{RPA}}(\mathbf{k}, \omega) = 1 - W_0(\tilde{\mathbf{k}}) \tilde{\pi}^{00}_{1\text{-loop}}(k_y, \omega), \tag{61}$$

and in the GRPA, it is defined by

$$\epsilon^{\text{GRPA}}(\mathbf{k}, \omega) = 1 - \frac{W_0(\tilde{\mathbf{k}}) \tilde{\pi}^{00}_{1\text{-loop}}(k_y, \omega)}{(1 + \tilde{W}_0(\tilde{\mathbf{k}}) \tilde{\pi}^{00}_{1\text{-loop}}(k_y, \omega))}. \tag{62}$$

4.2 Plasmon

Plasmon is the excitation mode associated with the charge fluctuation. The pole of the (G)RPA polarization function $\tilde{\pi}^{00}_{\text{(G)RPA}}$ is zero of $\epsilon^{\text{(G)RPA}}(\mathbf{k}, \omega)$. The plasmon appears at the outside range of the particle-hole continuum regime.

The difference of the plasmon behavior between k_x- and k_y-direction is the result of the spontaneously breaking the magnetic translation and rotation symmetry of the striped state. For the long wavelength limit and $\epsilon_{p_y+k_y} - \epsilon_{p_y} \ll \omega_p$, the plasma frequency ω_p rises like $k_y\sqrt{2\ln k_y}/|\mathbf{k}|^{1/2}$ for taking only $n = 0$ term. The origin of this gapless behavior is the Coulomb interaction $1/r$ in two dimensional space.

4.3 Correlation energy

Next we calculate the (G)RPA correlation energy,

$$E^{\rm total} = E^{\rm HF} + \int_0^1 d\lambda \frac{1}{2} \int_{-\infty}^{\infty} \frac{d^2k}{(2\pi)^2} \tilde{V}(\mathbf{k}) \langle E(\lambda) | \,\circ\!\!\circ\, \tilde{\rho}(\mathbf{k}) \tilde{\rho}(-\mathbf{k}) \,\circ\!\!\circ\, | E(\lambda) \rangle \quad (63)$$

where $\tilde{\rho}(\mathbf{k})$ is defined in Eq. (??) and $\tilde{V}(\mathbf{k}) = \frac{2\pi}{|\mathbf{k}|}$ is the Fourier transformed Coulomb interaction. The second term is the correlation energy. By replacing $\tilde{\rho}(\mathbf{k})$ with $\tilde{\rho}_*(\mathbf{k})$ and $\tilde{V}(\mathbf{k})$ with $V_l(\mathbf{k})$ in Eq. (63), the LL projected correlation energy is represented by a vNL basis:

$$\begin{aligned} E^{\rm corr} &= \frac{1}{2} \int_0^1 d\lambda \int_{-\infty}^{\infty} \frac{d^2k}{(2\pi)^2} V_l(\mathbf{k}) \langle E(\lambda) | \,\circ\!\!\circ\, \tilde{\rho}_*(\mathbf{k}) \tilde{\rho}_*(-\mathbf{k}) \,\circ\!\!\circ\, | E(\lambda) \rangle \\ &= \frac{1}{2} \int_0^1 d\lambda \int_{\rm MBZ} \frac{d^2k}{(2\pi)^2} \frac{d^2p_1}{(2\pi)^2} \frac{d^2p_2}{(2\pi)^2} \sum_n V_l(\tilde{\mathbf{k}} + 2\pi\tilde{\mathbf{n}}) e^{-\frac{i}{2\pi} k_x (p_1 - p_2)_y + i(\mathbf{p}_1 - \mathbf{p}_2) \times \mathbf{n}} \\ &\quad \times \langle E(\lambda) | b^\dagger_{l,\mathbf{p}_1+\mathbf{k}} b_{l,\mathbf{p}_1} b^\dagger_{l,\mathbf{p}_2} b_{l,\mathbf{p}_2+\mathbf{k}} | E(\lambda) \rangle. \end{aligned} \quad (64)$$

The integer n is caused by dividing the k-integral region into summation of one MBZ. The RPA contribution for the correlation energy is the sum of the bubble diagram as shown in Fig. which is derived by the perturbative calculation about the virtual coupling constant λ. The density correlation function

$$\begin{aligned} &\int_{\rm MBZ} \frac{d^2p_1}{(2\pi)^2} \frac{d^2p_2}{(2\pi)^2} \sum_n V_l(\tilde{\mathbf{k}} + 2\pi\tilde{\mathbf{n}}) e^{-\frac{i}{2\pi} k_x (p_1 - p_2)_y + i(\mathbf{p}_1 - \mathbf{p}_2) \times \mathbf{n}} \\ &\quad \times \langle E(\lambda) | b^\dagger_{l,\mathbf{p}_1+\mathbf{k}} b_{l,\mathbf{p}_1} b^\dagger_{l,\mathbf{p}_2} b_{l,\mathbf{p}_2+\mathbf{k}} | E(\lambda) \rangle \end{aligned}$$

$$\stackrel{\text{RPA}}{\simeq} \quad i\sum_{mnp}\pi^{(0)}_{mn}(k)W_n(\tilde{k})\pi^{(0)}_{np}(k)\lambda W_p(\tilde{k})\left(\frac{1}{1-\pi^{(0)}(k)\lambda W(\tilde{k})}\right)_{pm} \quad (65)$$

Here $\pi^{(0)}_{nm}$ is given in Eq. (??). For an easy estimate, we take only the diagonal matrix elements contribution

$$\text{Eq. (65)} \;\simeq\; i\sum_n(\pi^{(0)}_{nn}(k)W_n(\tilde{k}))^2\frac{\lambda}{1-\pi^{(0)}_{nn}(k)\lambda W_n(\tilde{k})} \quad (66)$$

In the summation about n, the contribution of $n \geq 1$ terms are negligible because of the Gaussian factor in $V_n(\tilde{\mathbf{k}})$. So we consider only the $n = 0$ term. The correlation energy, $E^{\text{corr}}_{\text{RPA}}$ in the RPA is written by $\epsilon^{\text{RPA}}(\mathbf{k},\omega)$ and $\tilde{\pi}^{00}(k_y,\omega)$ as

$$E^{\text{corr}}_{\text{RPA}} = -\frac{i}{2}\int_{-\infty}^{\infty}\frac{d\omega}{2\pi}\int_{\text{MBZ}}\frac{d^2k}{(2\pi)^2}\left\{\log\left(\epsilon^{\text{RPA}}(\mathbf{k},\omega)\right)+\tilde{\pi}^{00}(k_y,\omega)W_0(\tilde{k})\right\} \quad (67)$$

The numerical estimates of E^{HF}, the real part of $E^{\text{corr}}_{\text{RPA}}$ and the total energy E^{total} per particle at the half-filled $l = 2$ LL are obtained as follows:

$$E^{\text{HF}} = -0.7675 \quad (68)$$
$$E^{\text{corr}} = -0.0366 \quad (69)$$
$$E^{\text{total}} = -0.8041, \quad (70)$$

where the energy unit is $\frac{q^2}{a}$. Since the total energy is smaller than E^{HF}, the quantum fluctuations in the RPA is a significant contribution including the RPA plasmon.

In the GRPA, the summation of the diagram for the correlation energy is shown in Fig..and

$$i\sum_n(\pi^{(0)}_{nn}(k)W_n(\tilde{\mathbf{k}}))^2\frac{\lambda}{1-\pi^{(0)}_{nn}(k)\lambda W^{\text{eff}}_n(\tilde{\mathbf{k}})}.$$

Hence, the correlation energy $E^{\rm corr}_{\rm GRPA}$ in the GRPA is written by $\epsilon^{\rm GRPA}(\mathbf{k},\omega)$ and $\tilde{\pi}^{00}(k_y,\omega)$ as

$$
\begin{aligned}
E^{\rm corr}_{\rm GRPA} &= -\frac{i}{2}\int_{-\infty}^{\infty}\frac{d\omega}{2\pi}\int_{\rm MBZ}\frac{d^2k}{(2\pi)^2}\left\{\left(\frac{W_0(\tilde{k})}{W_0^{\rm eff}(\tilde{k})}\right)^2\log\left(1-W_0^{\rm eff}(\tilde{k})\tilde{\pi}^{00}(k_y,\omega)\right)\right. \\
&\quad \left. +\tilde{\pi}^{00}(k_y,\omega)\frac{\{W_0(\tilde{k})\}^2}{W_0^{\rm eff}(\tilde{k})}\right\}. \qquad (71)
\end{aligned}
$$

The numerical estimates of the real part of $E^{\rm corr}_{\rm GRPA}$ and the total energy $E^{\rm total}$ per particle at the half-filled $l = 2$ LL are obtained as follows:

$$
\begin{aligned}
E^{\rm corr} &= -0.0523 \qquad (72)\\
E^{\rm total} &= -0.8198. \qquad (73)
\end{aligned}
$$

Yoshioka's HF energy of the anisotropic charge density wave (ACDW) (with a full gap of order 1K):

$$E^{\rm Y} = -0.7763. \qquad (74)$$

Shibata and Yoshioka 's density matrix renormalization group (DMRG) method (stripe):

$$E^{D} = -0.796 \pm 0.004. \qquad (75)$$

ACDW is insulator in x and y-direction and the gap structure causes the quantization of the Hall conductance,which is different from experiment.

5 Current activation from undercurrent:on precise determination of the fine structure constant

5.1 Implications of gas of negative pressure

Unusual thermodynamic properties: negative pressure and negative compressibility.

Quantum Hall gas shrinks and electric charge density becomes nonuniform.

5.2 Current activation from undercurrent as a new tunneling mechanism

The Fermi energy is in a higher Landau level and lower Landau levels are filled completely and one Landau level is partially filled. The induced current in the partially filled highest Landau level,

$$\begin{aligned} j_{\rm ind} &= V_l e^{\beta(E_l-\mu)} \sinh \frac{\beta e E_H^{\rm eff}}{2}, \\ V_l &= \frac{4\pi\nu' q^2 \pi^{3/2}}{a^2(l+1)} \int_0^\infty dx x^{1/2} \{L_l^{(1)}(x)\}^2 e^{-x} \end{aligned} \tag{76}$$

, where $E_H^{\rm eff}$ is the effective Hall field.

The total longitudinal resistance,

$$R_{xx} = R_{xx}^{(s)} e j_{\rm ind}/\sigma_{xy} E_H, \tag{77}$$

$$R_{xx}^{(s)} = (\frac{e^2}{h})^{-1} \tag{78}$$

where $R_{xx}^{(s)}$ is the longitudinal resistence of the stripe state. The experiment of Kawaji et al[?].

5.3 Dissipative QHR

The resistivities at low temperature,

$$\begin{aligned} \rho_{xx} &= \tilde{\rho} e^{-\beta \Delta E_{\text{gap}}}, \\ \rho_{xy} &= (\frac{e^2}{h} N)^{-1}, \\ \Delta E_{\text{gap}} &= \mu - E_l - e E_H^{\text{eff}} a/2, \end{aligned} \tag{79}$$

where $\tilde{\rho}$ is temperature independent.

Thus ρ_{xy} is quantized even though ρ_{xx} does not vanish.

5.4 Precise determination of the fine structure constant from IQHE

The unusual properties of the Hall gas

→

quantum Hall gas has a tendency to shrink and the electric property of some spatial region is determined only from that region. Even though an energy dissipation occurs in some region of the sample, the other part of the same sample which is completely occupied by the localized electron could give the exactly quantized value of the Hall conductance.

→

The Hall conductance measured in this part of the sample is quantized exactly.

→

In fact there is a small energy dissipation in the real measurement from the current contact area because there is a potential drop in the direction parallel to the current.

However it is possible to measure the fine structure constant precisely from the IQHE.

6 Summary

The precise measurement of fundamental physical constants such as the light velocity,the electron charge, the Plank constant and their combinatios ,the fine structure constant, α is important.

Since the most accurate value of α is obtained from the quantum Hall effect,it is necessary to know if the precise value of α is known from the quantum Hall effect.

Formulation based on von Neumann lattice representaion of guiding center variables is such method that makes derivation of rigorous identities and study of many body effects transparent.

We give the proof of the integer quantization of the Hall conductance and we develope the mean field theory of the anisotropic quantum Hall gas based on this formalism.

Reference

K. Ishikawa, T. Aoyama, Y. Ishizuka, and N. Maeda, *Int. Jour. Mod. Phys.*B **17**,4765(2003).cond-mat/0309163.

M. P. Lilly, K. B. Cooper, J. P. Eisenstein, L. N. Pfeiffer, and K. W. West, *Phys. Rev. Lett.* **82**, 394 (1999); R. R. Du, D. C. Tsui, H. L. Stormer, L. N. Pfeiffer, K. W. Baldwin, and K. W. West, *Solid State Communications*. **109**, 389 (1999).

K. Ishikawa, N. Maeda, T. Ochiai, H. Suzuki, *Physica* **4 E**, 37 (1999).

N. Imai, K. Ishikawa, T. Matsuyama, and I. Tanaka, *Phys. Rev.* **B 42**, 10610 (1990).

K. Ishikawa, N. Maeda, T. Ochiai, *Phys. Rev. Lett.* **82**, 4292 (1999); N. Maeda, *Phys. Rev.* **B 61**, 4766 (2000); K. Ishikawa and N. Maeda, *Physica* **B 298**, 159 (2001); T. Aoyama, K. Ishikawa and N. Maeda,*Europhys. Lett.* **59**, 444 (2002); T. Aoyama, K. Ishikawa, Y. Ishizuka and N. Maeda,*Phys. Rev.* **B 66**, 155319 (2002).

A. A. Koulakov, M. M. Fogler, and B. I. Shklovskii, *Phys. Rev. Lett.* **76**, 499 (1996); M. M. Fogler, A. A. Koulakov, and B. I. Shklovskii,*Phys. Rev.* **B 54**, 1853 (1996).

R. Moessner and J. T. Chalker, *Phys. Rev.* **B 54**, 5006 (1996).

S. Kawaji, J. Iizuka, T. Shimada, H. Iizuka, T. Kuga, amd T. Okamoto, *J. Phys. Soc. Jpn.* **67**, 1110 (1998); S. Kawaji, H. Iizuka, T. Kuga, and T. Okamoto, *Physica* **B**

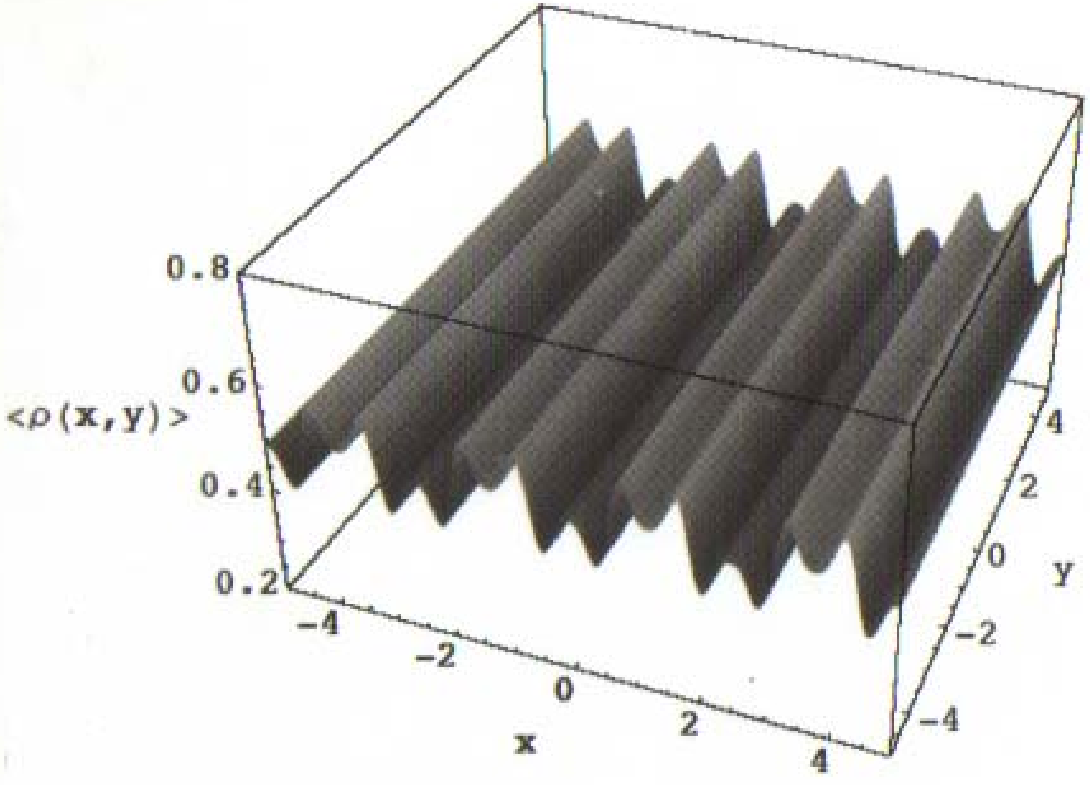

0.8
0.6
0.4
0.2
<ρ(x,y)>
-4
-2
0
2
4
x
y

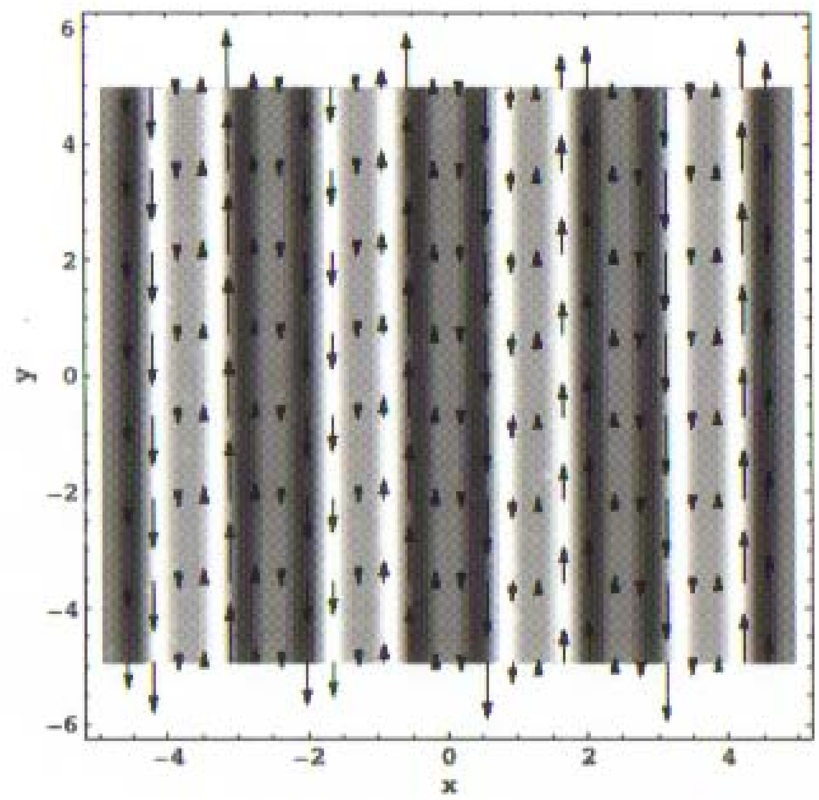

6
4
2
0
-2
-4
-6
y
x

I. FIGURES

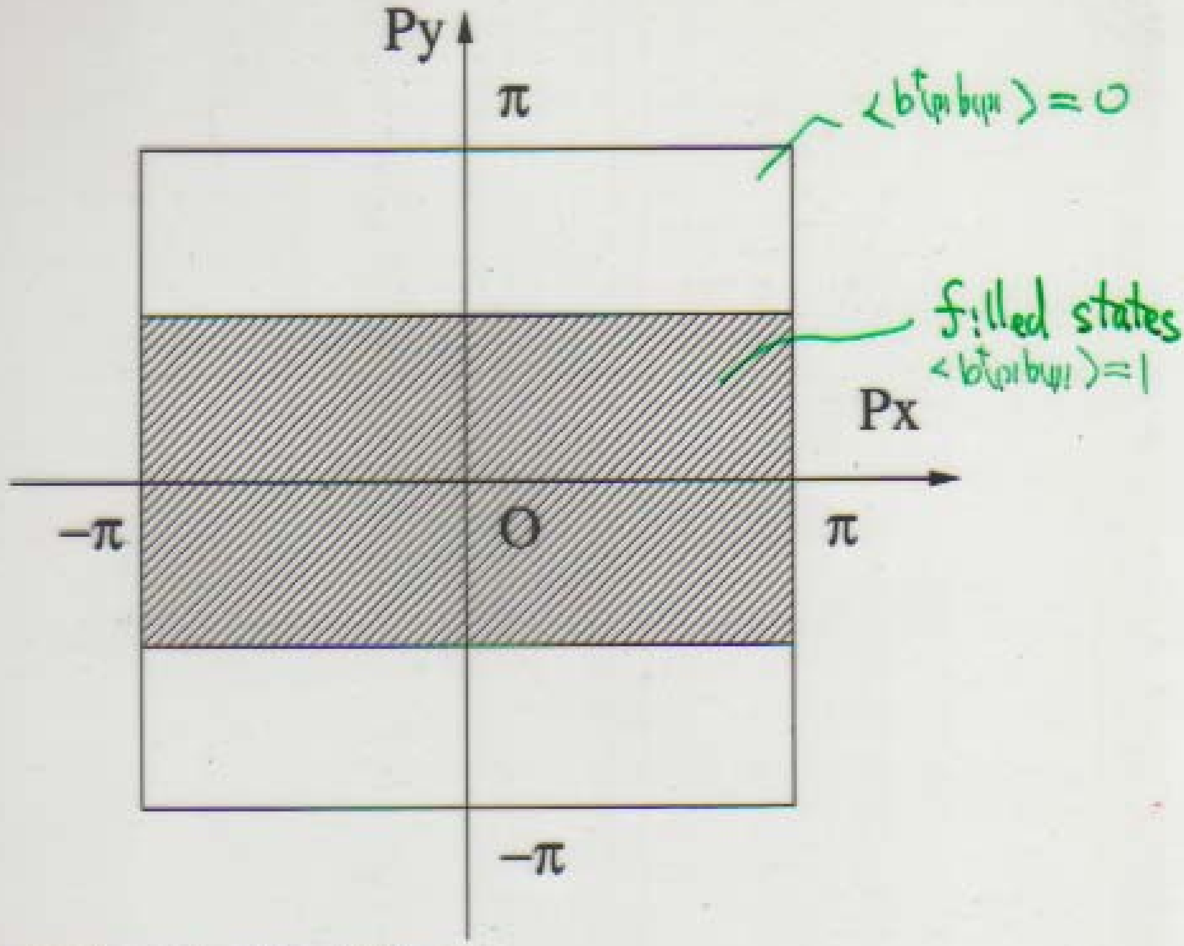

Fig. 1. The Fermi sea for the K_x invariant Hall gas state.

- one particle energy $\epsilon(p_y, \nu)$
- $\vec{K}$ symmetry $\begin{cases} \vec{p} \to \vec{p} + K_x & \text{conserved} \\ \vec{p} \to p + K_y & \text{broken} \end{cases}$
- P_x direction ≈ integer Hall effect ≈ hard
  P_y direction ≈ Fermi gas ≈ soft
- $\sigma_{xx} = 0$ Landau level's gap
  $\sigma_{yy} = \frac{e^2}{h}$ one dimensional channel.

$\Delta R_H/R_H$ and ρ_{xx} vs I (injected current)

Iizuka et al. (2000), 0.35 K

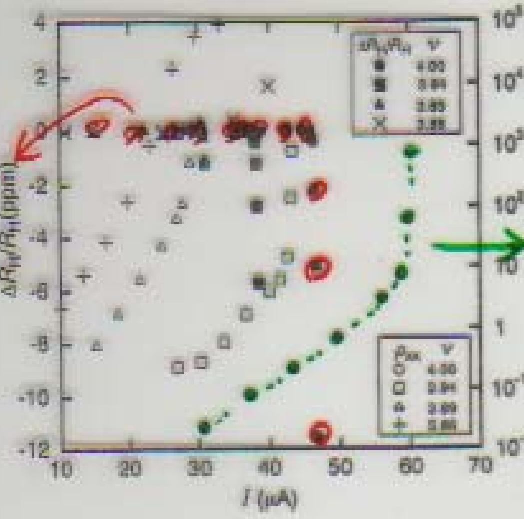

Fig. 1. Deviation of the Hall resistance from the quantized value $R_H(4)$ given by $\Delta R_H/R_H$ and the diagonal resistivity ρ against the current I at filling factors ν equal to and smaller than 4.

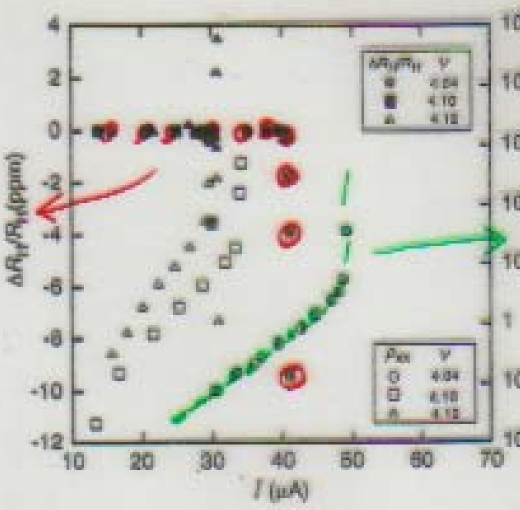

Fig. 2. Deviation of the Hall resistance from the quantized value $R_H(4)$ given by $\Delta R_H/R_H$ and the diagonal resistivity ρ against the current I at filling factors ν larger than 4.

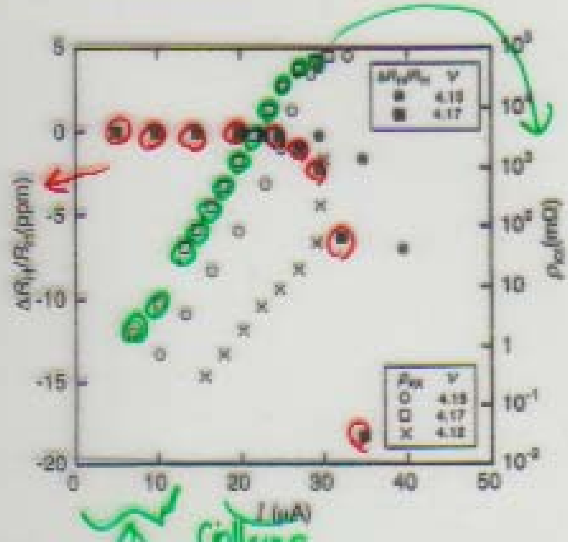

Fig. 3. Deviation of the Hall resistance from the quantized value $R_H(4)$ given by $\Delta R_H/R_H$ and the diagonal resistivity ρ against the current I at filling factors $\nu = 4.15$ and 4.17 do not show critical behavior. The critical behavior of the diagonal resistivity at $\nu = 4.12$ is shown for comparison.

dissipative quantum Hall regime

(1998)

S. Kawaji et al. / Phys.

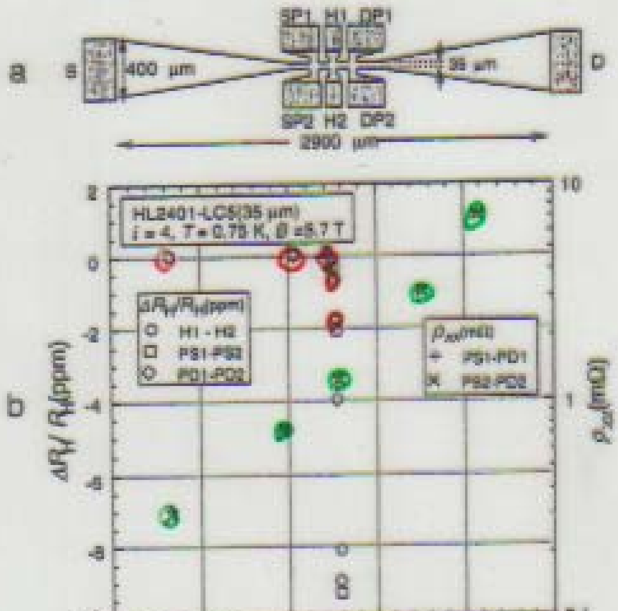

Fig. 1. (a) Electrode structure of a butterfly-type Hall bar. Shaded areas are metal ohmic electrodes. Length of the central parallel part: 600 μm. Distance between adjacent voltage probe centers: 150 μm. Probe width: 50 μm. (b) Deviation of the Hall resistance ΔR_H from the quantized value R_H ($\nu = 4$) and diagonal resistivity ρ_{xx} against current I_{SD}. ρ_{xx} is calculated by $\rho_{xx} = R_{xx} w/l$ where R_{xx} is measured across SP1 and DP1, or SP2 and DP2.

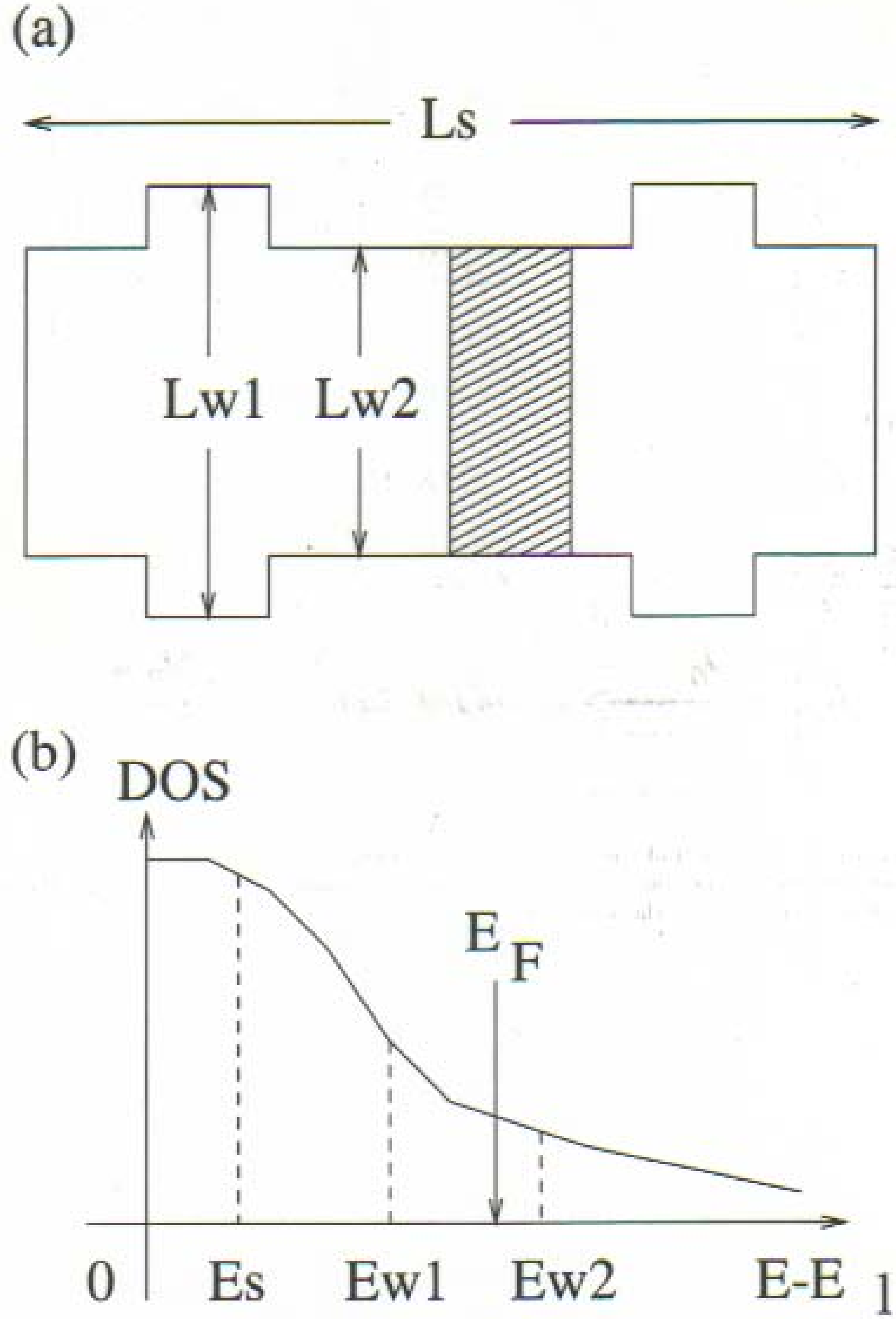

Fig. 9. A typical wave function in the configuration space (shaded region in (a)) and energy region in the density of states (DOS) in (b). The Fermi energy is in the dissipative QHR and the compressible state extends to the potential probe regions.

current in isolated strip.　K. I and Maeda, Cond-mat. 0102347

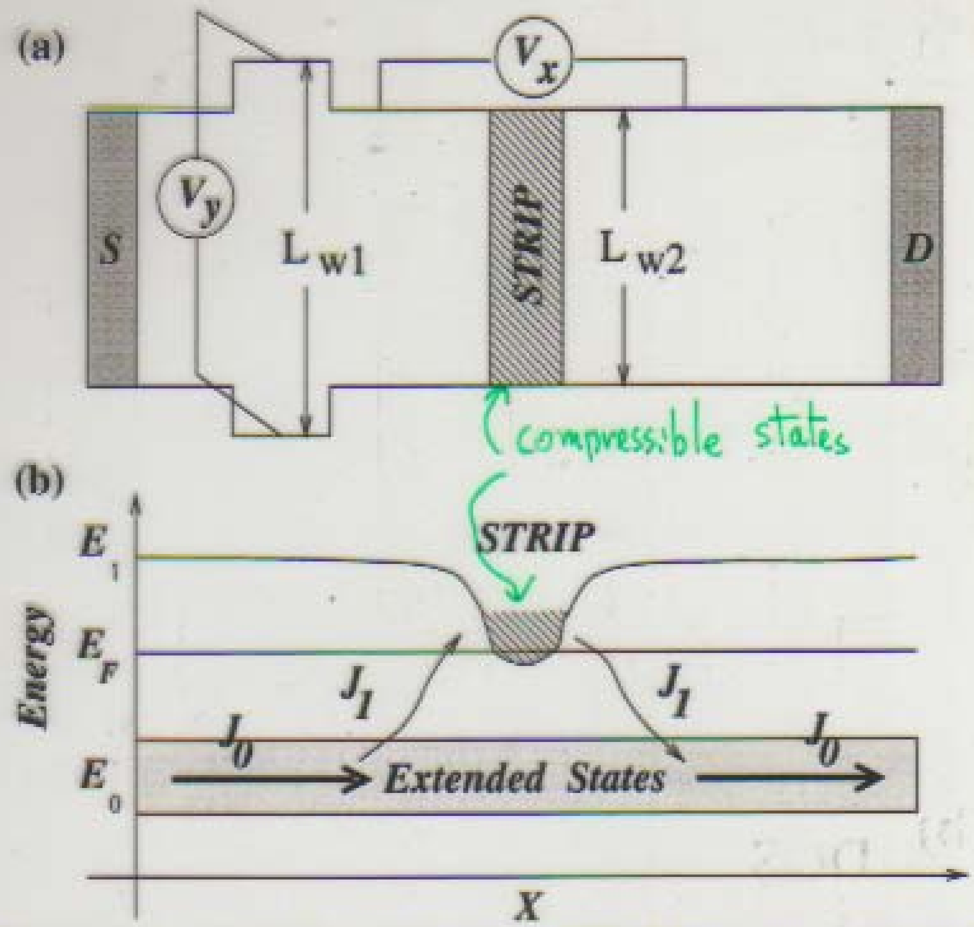

Fig 10. (a) Schematical view of a Hall bar in the dissipative QHR. Electric current is injected from S to D. (b) Sketch of the extended states carrying the undercurrent J_0 and the compressible state carrying the induced current J_1 at the strip region in the energy and the x-position.

strip :

disconnected from S, D region.

current in the strip (J_I) is from current in Extended states, by tunneling.

$$J_1 = \int \frac{d^2p}{(2\pi)^2} d\vec{k} \, \frac{V(\vec{k})}{2} \, |f_{l_1 l_2}(\vec{k})|^2 v_x \, e^{\beta \delta E_1(\vec{p}-a\vec{k})}$$

$$v_x = \frac{E_H}{B}, \quad \beta = \frac{1}{kT}, \quad \delta E_1(p-ak) = E_l + \gamma e E_H \frac{a^2}{2\pi}(\vec{p}_1 - a\hat{k}) - E_F < 0$$

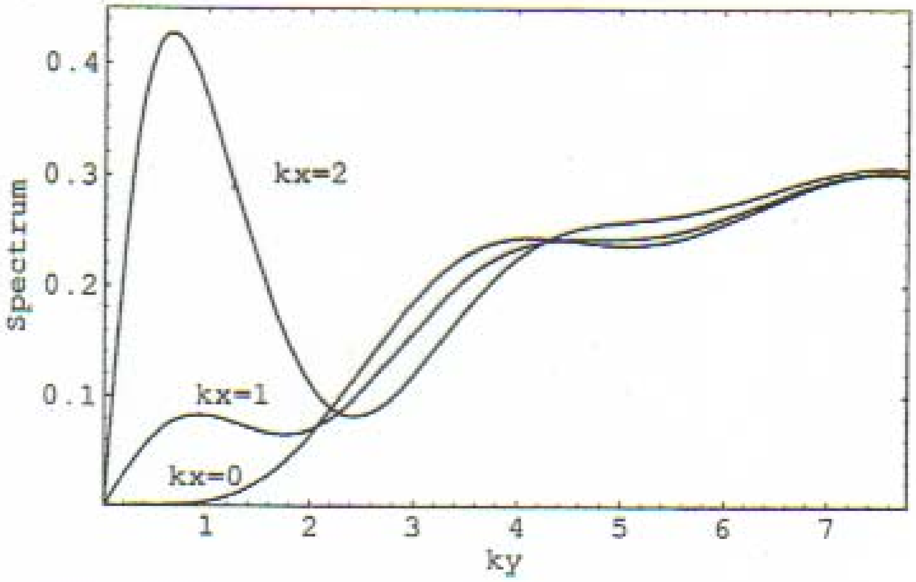

FIG. 4. Enlarged picture of the energy spectrum Δ at $0<k_y<\pi r_s$ for $k_x=0,1,2,\nu=2+1/2$ in the single-mode approximation.

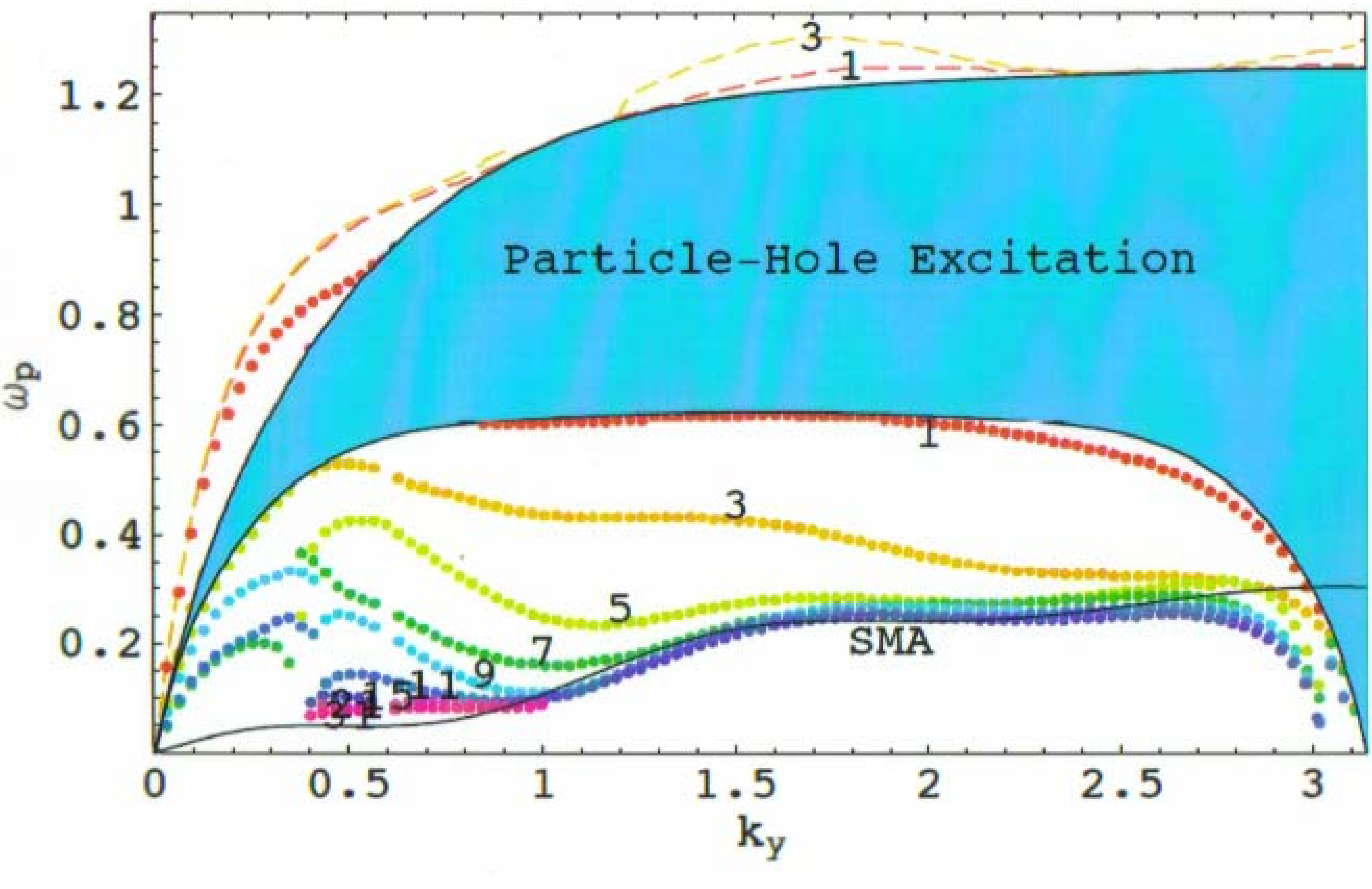

Particle-Hole Excitation
SMA
ω_p
k_y
1.2
1
0.8
0.6
0.4
0.2
0
0.5
1.5
2
2.5
3
5
7
9
11
15
21
31

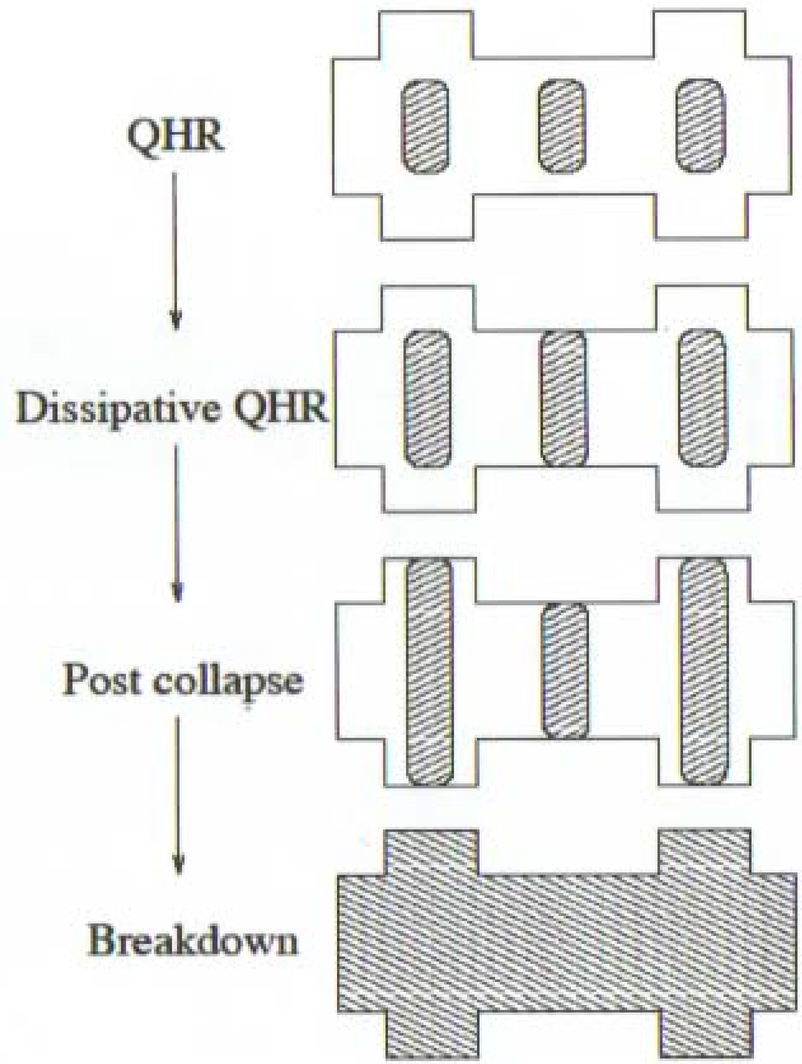
QHR
Dissipative QHR
Post collapse
Breakdown

M.P. Lilly et al. (1999) Anisotropic states $\nu \geq 9/2$

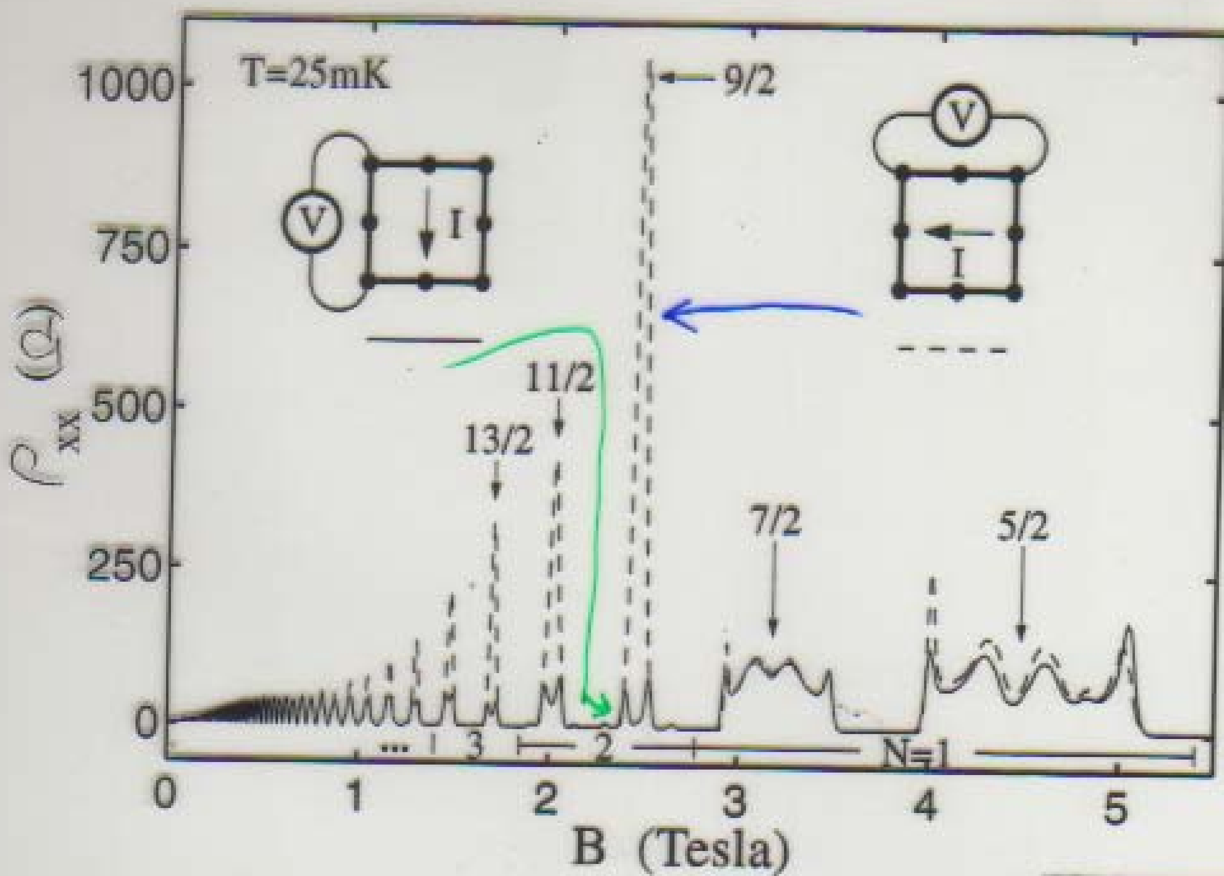

W. Pan et al. (1999)

pairing state

$\nu = 5/2$

CDW ?

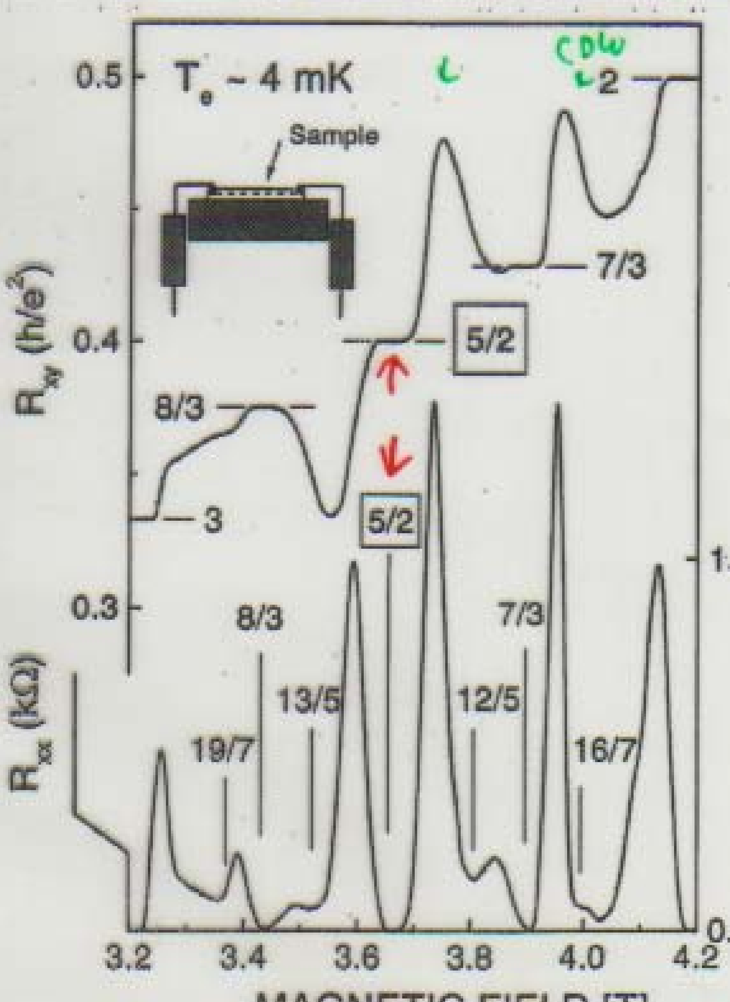

FIG. 1. Hall resistance R_{xy} and longitudinal resistance R_{xx} at

Fractional Hall Effect, overview of Experiments ①

ICHEP 2
MIT 3

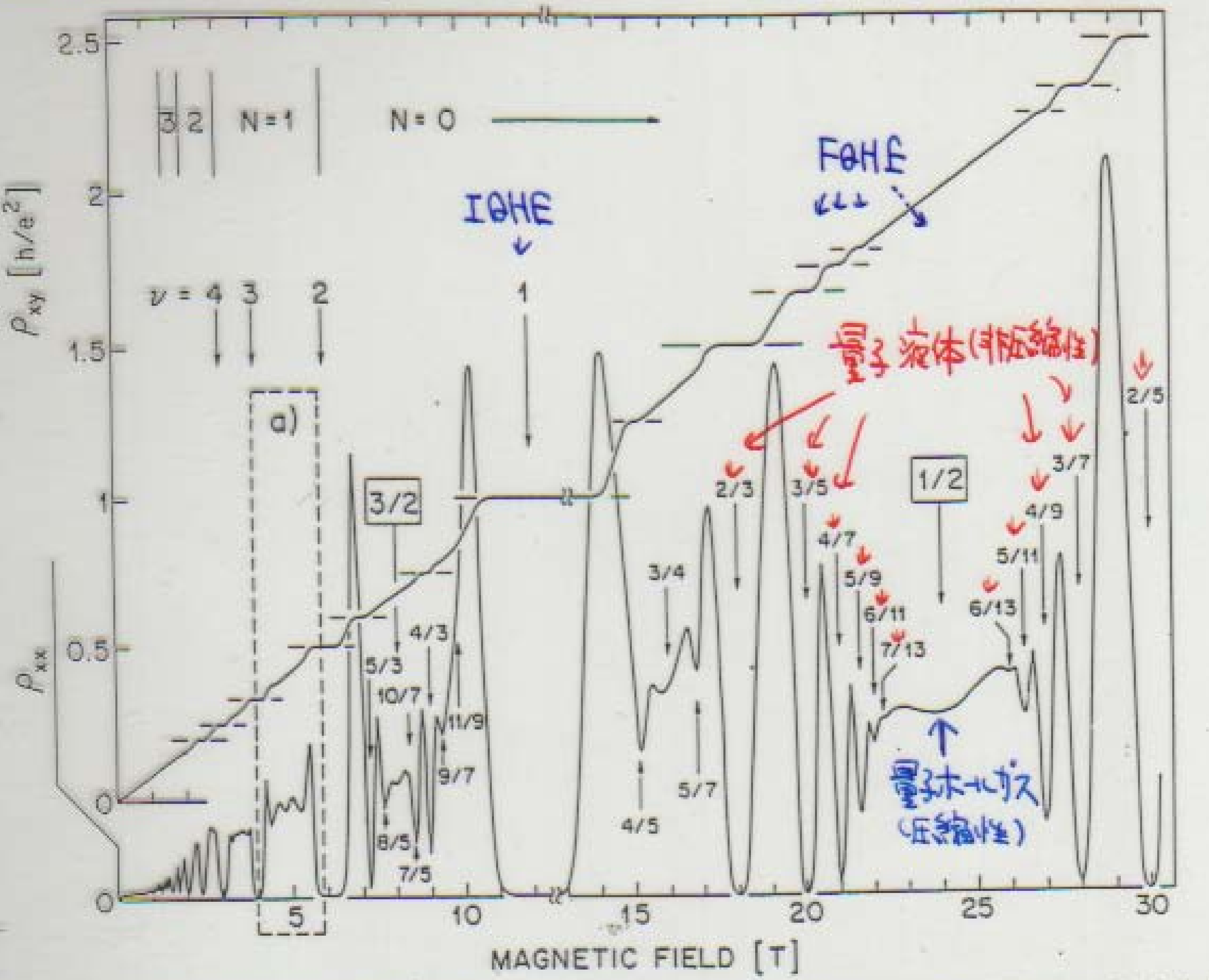

Overview of diagonal resistivity ρ_{xx} and Hall resistance ρ_{xy} of sample described in text. The use of a hybri-
ield required composition of this figure from four different traces (breaks at ≈12 T). Temperatures were
: high-field Hall trace at $T = 85$ mK. The high-field ρ_{xx} trace is reduced in amplitude by a factor 2.5 for c
l Landau levels N are indicated.

QHE

$$\begin{cases} \rho_{xx} = 0 = \sigma_{xx}^{-1} \\ \rho_{xy} = \left(\frac{e^2}{h}\ \frac{\xi}{p}\right)^{-1} = \sigma_{xy}^{-1} \end{cases}$$

$$\begin{pmatrix} V_x \\ V_y \end{pmatrix} = \begin{pmatrix} \rho_{xx} & \rho_{xy} \\ \rho_{yx} & \rho_{yy} \end{pmatrix} \begin{pmatrix} I_x \\ 0 \end{pmatrix}$$

$$\begin{pmatrix} I_x \\ 0 \end{pmatrix} = \begin{pmatrix} \sigma_{xx} & \sigma_{xy} \\ \sigma_{yx} & \sigma_{yy} \end{pmatrix} \begin{pmatrix} V_x \\ V_y \end{pmatrix}$$

pressure and compressibility: 量子ホールガスの圧力，圧縮率（石川–前田 理論計算）

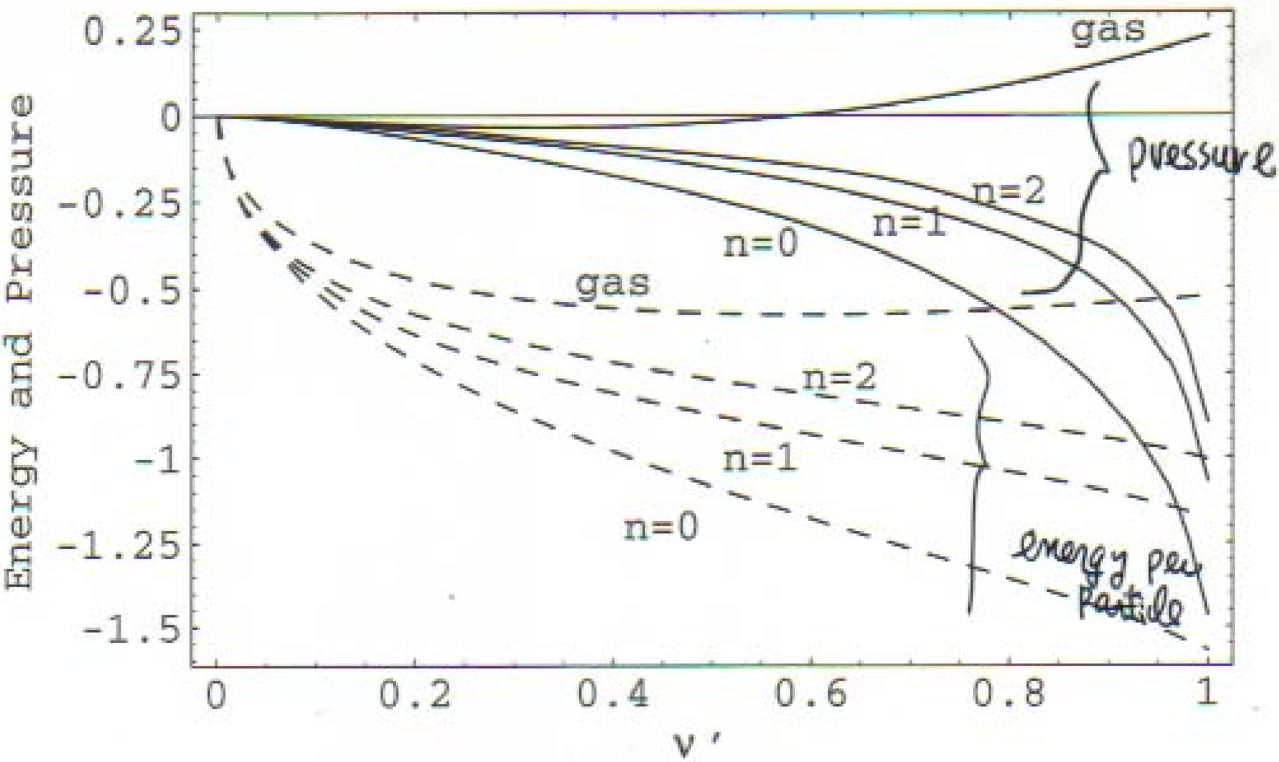

Fig 2. Energy per particle (dashed lines) in the unit of q^2/a and pressure (solid line) in the unit of q^2/a^3 for the filling factor $\nu = n + \nu'$. Corresponding values for the two-dimensional electron gas without magnetic field are also shown (gas) at density$= \nu'/a^2$ for $B = 6$T in GaAs.

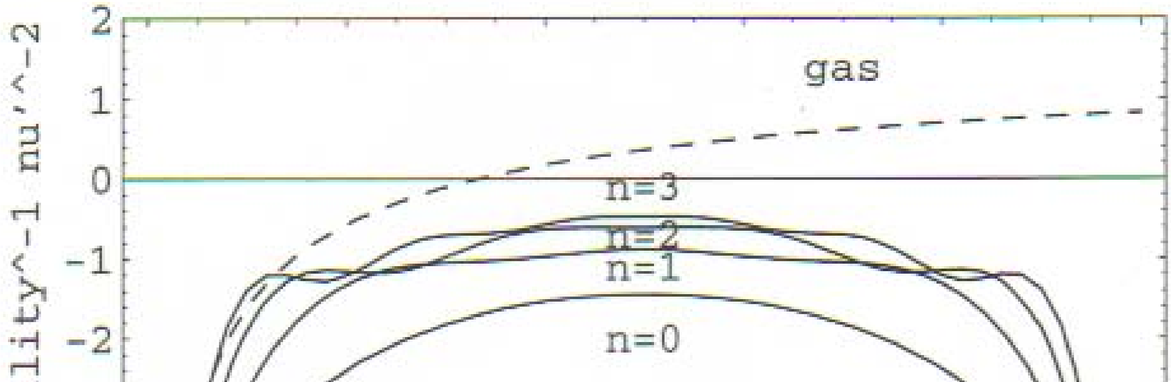

Fig 3. Inverse compressiblity times ν'^{-2} in the unit of q^2/a^3 for $\nu = n+\nu'$. Dashed line shows the corresponding value of the two-dimensional electron gas without magnetic field (same as Fig. 2).

Hartree-Fock potential :

$$v_{HF}(\vec{p}) = \sum_{\vec{N}} \left\{ v_e(2\pi\vec{N})\, e^{i\,\vec{p}\times\vec{N}} - v_e(2\pi\vec{N}-\vec{p}) \right\}$$

↙ Fourier transform

$$= \sum_{\vec{N}'} \tilde{v}_e(\vec{p}+\vec{N}') - \sum_{\vec{N}} v_e(2\pi\vec{N}-\vec{p})$$

exchange force direct force

charge density

$$\langle \rho(\vec{x}) \rangle = \int \frac{d^2k}{(2\pi)^2} e^{i\vec{k}\vec{x}} \int_{BZ} \frac{d^2p}{(2\pi)^2} \langle b_\ell^\dagger(\vec{p})\, b_\ell(\vec{p}+q\hat{k}) \rangle$$

$$\langle f_\ell | e^{-i(k_x\xi + k_y Y)} | f_\ell \rangle\, e^{i\frac{q}{4\pi}\hat{k}_x(2\hat{p}_y + q\hat{k}_y)}$$

$$\langle b_\ell^\dagger(\vec{p})\, b_\ell(\vec{p}+q\hat{k}) \rangle = \sum_N \Theta\left(\frac{\pi}{2} - |p_y|\right) \delta(\vec{k} - 2\pi\vec{N})\, e^{i(N_x - N_y)\pi - iN_y p_x}$$

$$= \int \frac{d^2k}{(2\pi)^2} e^{i\vec{k}\vec{x}}\, \delta(\vec{k} - 2\pi\vec{N}) \int_{BZ} \frac{d^2p}{(2\pi)^2} \Theta\left(\frac{\pi}{2} - |p_y|\right)$$

$$e^{i(N_x N_y + N_x - N_y)\pi}\; e^{i(N_x p_y - N_y p_x)}$$

$$= \int \frac{d^2k}{(2\pi)^2} e^{i\vec{k}\vec{x}}\, \delta(\vec{k} - 2\pi\vec{N})\, \delta_{N_y,0} \int \frac{dp_y}{2\pi} \Theta\left(\frac{\pi}{2} - |p_y|\right)$$

$$e^{iN_x\pi + iN_x p_y}$$

$$= \left(\frac{1}{2\pi}\right)^2 \sum e^{i2\pi N_x x} \int \frac{dp_y}{2\pi} \Theta\left(\frac{\pi}{2} - |p_y|\right) e^{iN_x(\pi + p_y)}$$

Periodic function of x.

Quantum Hall Effects (Experiments) (recent)

properties

- Integer quantum Hall effects : incompressible (energy gap $\neq 0$)

$$\sigma_{xy} = \frac{e^2}{h} \cdot N$$

$$\sigma_{xx} = 0$$

"Metrology", SIN unit "α"

- Fractional quantum Hall effects : incompressible liquid

$$\sigma_{xy} = \frac{e^2}{h}\frac{q}{p}$$

$$\sigma_{xx} = 0$$

"Laughlin variational wave function"

"composite fermion"

- anisotropic compressible Hall gas state : compressible gas (energy gap $= 0$)

$$\sigma_{xx} \gg \sigma_{yy}$$

$$\nu = 3 + \frac{1}{2}, 4 + \frac{1}{2}, \cdots$$

- pairing states : incompressible

superconductor ?

$$\nu = \frac{5}{2}$$

P flaton

P-wave superconductor

- reentrant Charge Density Wave states (CDW) : incompressible

$$\sigma_{xy} = \frac{e^2}{h} \tilde{N}$$

$$\sigma_{xx} = 0$$

many phases (ground states) are realized. There are many unsolved proplems. Metrology, compressible Hall gas are discussed here.

One particle kinetic energy of Quantum Hall gas.

$\nu = l + \frac{1}{2}$